



# Methodology to separate channel conductions of two level vertically stacked SOI nanowire MOSFETs

Bruna Cardoso Paz<sup>a,\*</sup>, Mikaël Cassé<sup>b</sup>, Sylvain Barraud<sup>b</sup>, Gilles Reimbold<sup>b</sup>, Maud Vinet<sup>b</sup>, Olivier Faynot<sup>b</sup>, Marcelo Antonio Pavanello<sup>a</sup>

<sup>a</sup> Department of Electrical Engineering, Centro Universitário FEI, São Bernardo do Campo, Brazil

<sup>b</sup> Département des Composants Silicium – SCME/LCTE, CEA-LETI Minatex, Grenoble, France

## ARTICLE INFO

The review of this paper was arranged by Prof. S. Cristoloveanu

### Keywords:

Vertically stacked nanowires  
SOI  
Mobility  
Back gate bias  
Tridimensional numerical simulations  
Temperature

## ABSTRACT

This work proposes a new method for dissociating both channel conductions of two levels vertically stacked inversion mode nanowires (NWs) composed by a Gate-All-Around (GAA) level on top of an  $\Omega$ -gate level. The proposed methodology is based on experimental measurements of the total drain current ( $I_{DS}$ ) varying the back gate bias ( $V_B$ ), aiming the extraction of carriers' mobility of each level separately. The methodology consists of three main steps and accounts for  $V_B$  influence on mobility. The behavior of non-stacked  $\Omega$ -gate NWs are also discussed varying  $V_B$  through experimental measurements and tridimensional numerical simulations in order to sustain proposed expressions of mobility dependence on  $V_B$  for the bottom level of the stacked structure. Lower mobility was obtained for GAA in comparison to  $\Omega$ -gate. The procedure was validated for a wide range of  $V_B$  and up to 150 °C. Similar temperature dependence of mobility was observed for both  $\Omega$ -gate and GAA levels.

## 1. Introduction

Multiple gate MOSFETs have attracted the interest of semiconductor industry due to strong immunity against short channel effects and great scalability because of improved electrostatic coupling [1–3].  $\Omega$ -gate and GAA MOSFETs with nanoscale cross-section, also denominated as nanowires, turned into candidates for future technological nodes due to their performance [2,4]. Such devices are fabricated with close dimensions for both silicon thickness ( $H_{FIN}$ ) and fin width ( $W_{FIN}$ ), around 10 nm. In order to fulfill higher drive current requests and increase the on-state current by footprint ( $I_{ON}/W_{FIN}$ ), nanowires have been recently vertically stacked thanks to advances on tridimensional integration process [5–7]. Once vertically stacked NWs present overall channel width ( $W_{eff}$ ) proportional to the number of stacked levels (or beams), these devices have higher aspect ratio, which is necessary for NWs to reach industrial targets for saturation current [8].

The implementation of vertically stacked NWs brings technological challenges such as the reduction of intrinsic parasitic capacitance and integration of carriers' mobility boosters. These problems have been recently addressed by the innovative structure fabricated at CEA-LETI, combining inner spacers and SiGe source/drain in vertically stacked p-type NW MOSFETs [7]. The overall effective mobility of these stacked NWs was investigated in [9], while [10] presented a methodology to

perform individual electrical characterization of each NW level including explicit expressions for the low field mobility ( $\mu_0$ ) and mobility degradation coefficients ( $\theta_1$  and  $\theta_2$ ) dependence on  $V_B$ . Once the first work aiming to separate the channel conductions of stacked multiple gate devices using  $V_B$  [11] does not take into account transport parameters dependence on the back bias, the methodology proposed in [10] improves [11]. In this work, we extend [10] by including experimental measurements and tridimensional numerical simulations of non-stacked  $\Omega$ -gate NWs varying  $V_B$  in order to explain physical effects in the potential, electric field and holes mobility under different back bias conditions. Such explanations are important to understand the vertically stacked NWs behavior and, therefore, sustain the expressions used for mobility dependence on  $V_B$  in the proposed methodology, once the bottom level of the stacked structure is  $\Omega$ -shaped. Moreover, this work brings deeper details of the proposed methodology step by step, so it can be easily reproduced. Discussions concerning temperature influence on  $V_B$  dependence are also presented in this work.

The paper is organized as follows: Section 2 details the devices characteristics for both stacked (Section 2.1) and non-stacked NWs (Section 2.2). Section 3 presents the main physical effects of applying  $V_B$  on mobility of non-stacked  $\Omega$ -gate NWs (Section 3.1), the proposed methodology to dissociate channel conductions of two levels vertically stacked NWs (Section 3.2) and temperature influence on  $V_B$  dependence

\* Corresponding author.

E-mail address: [bcpaz@fei.edu.br](mailto:bcpaz@fei.edu.br) (B.C. Paz).

<https://doi.org/10.1016/j.sse.2018.08.012>

Received 21 May 2018; Received in revised form 4 August 2018; Accepted 30 August 2018

Available online 31 August 2018

0038-1101/ © 2018 Elsevier Ltd. All rights reserved.

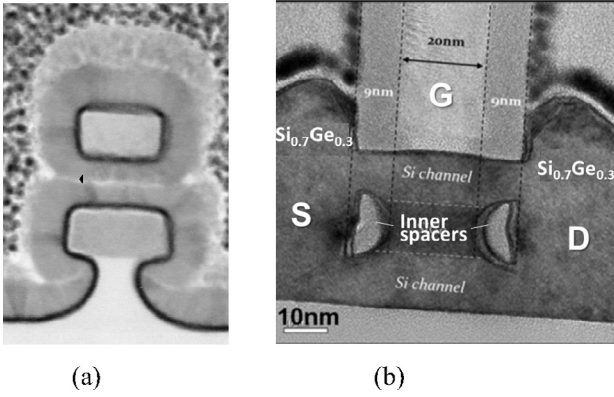


Fig. 1. Vertically stacked SOI nanowire cross section (a) and longitudinal section (b) TEM images.

(Section 3.3). Finally, Section 4 points out the main conclusions of this work.

## 2. Devices characteristics

### 2.1. Vertically stacked NWs

Transistors are [1 1 0]-oriented vertically stacked p-type inversion mode nanowires MOSFETs with two levels, being the bottom level  $\Omega$ -gated and the top level GAA. Fig. 1 shows Transmission Electron Microscopy (TEM) images of the studied stacked NWs cross section (a) and the longitudinal section (b). Usually the vertically stacked NWs have an  $\Omega$ -gated bottom level while the upper levels are GAA because the fabrication process starts from Fully Depleted (FD) SOI wafers. The first Si channel lies on top of the buried oxide and the upper channels are fabricated on top of SiGe layers, which are replaced after selective etching, giving place to the surrounded gate stack of GAA NWs. From Fig. 1a, it is possible to note that the front gate of the bottom NW is electrostatically coupled with the back gate. Although narrow triple gate MOSFETs present lower back gate bias ( $V_B$ ) influence in comparison to planar MOSFETs [12], the potential lines coming from the back gate manage to reach the Si channel through the interface between Si and buried oxide. On the other hand, the top NW is independent of  $V_B$  because it is surrounded by the gate stack. Despite the lower impact of  $V_B$  over the electrical parameters of narrow  $\Omega$ -NWs, since the bottom NW is  $V_B$  dependent while the top one is  $V_B$  independent, back biasing can be used as a tool to separate the channels conduction. The interest of using back bias in this work is attached to the methodology proposed in Section 3 to perform individual electrical characterization for future technology optimization.

Devices have been fabricated at CEA-LETI, starting from Silicon-On-Insulator (SOI) wafers with 145 nm buried oxide thickness ( $t_{\text{BOX}}$ ) and using a replacement metal gate (RMG) process to obtain a gate stack composed by  $\text{HfO}_2/\text{TiN}/\text{W}$ , resulting in effective oxide thickness (EOT) of 1.15 nm. Each level has a 10 nm thick undoped Si channel and both levels are attached by common metal gate and  $\text{Si}_{0.7}\text{Ge}_{0.3}:\text{B}$  raised source/drain (B doping level in the order of few  $10^{20} \text{ cm}^{-3}$  [13]). The transistors have been fabricated in multi finger structures with 50 fins in parallel and channel length (L) of 100 nm. Further fabrication details of the stacked-NWs studied in this work can be found in [7].

Fig. 2 presents drain current,  $I_{\text{DS}}$  (a), transconductance,  $g_m$  (b), and its derivative,  $\delta g_m / \delta V_{\text{GS}}$  (c), as a function of the front gate voltage ( $V_{\text{GS}}$ ) for stacked NW with  $W_{\text{FIN}} = 15 \text{ nm}$  and  $L = 100 \text{ nm}$ , at low drain voltage ( $V_{\text{DS}} = -40 \text{ mV}$ ), varying  $V_B$  from  $-90 \text{ V}$  to  $90 \text{ V}$ . In these figures the curves with symbols refer to  $V_B = 0 \text{ V}$ . During the measurements,  $V_B$  was applied at the substrate of the whole wafer, which is isolated from the active channels by the thick buried oxide. Although  $\pm 90 \text{ V}$  may seem like extremely high bias condition, it is important to

remember that  $t_{\text{BOX}} = 145 \text{ nm}$ . For simplicity, considering the same linear potential drop across the front and back interfaces,  $90 \text{ V}$  applied at  $145 \text{ nm}$ -thick oxide would correspond to  $\sim 0.7 \text{ V}$  applied at the same oxide with thickness of  $1.15 \text{ nm}$ . The applied back bias values must be adjusted according to the technology of the studied SOI MOSFET to avoid reliability and degradation issues due to high vertical electric field.

Fig. 2a shows expected shift of curves to the left as  $V_B$  increases due to threshold voltage ( $V_{\text{TH}}$ ) variation. Moreover, small back conduction is noted in the subthreshold region of logarithmic curves for negative back gate values.

Fig. 2b shows two distinguished peaks for  $g_m$  depending on  $V_B$ . Results suggests some  $V_{\text{TH}}$  mismatch between bottom and top levels once the two peaks are still slightly perceived at  $V_B = 0 \text{ V}$ , the first for  $V_{\text{GS}} \cong -0.4 \text{ V}$  and the second for  $V_{\text{GS}} \cong -0.75 \text{ V}$ . Two effects are observed and overlapped. First, the  $g_m$  peak decreases with  $V_B$  increase for negative values (dashed lines) and for high positive  $V_B$  (higher than  $50 \text{ V}$ ). Second, for sufficiently low  $V_B$  a second  $g_m$  peak appears at higher  $V_{\text{GS}}$  voltages. This second  $g_m$  peak presents the opposite behavior from  $0 \text{ V} < V_B < 50 \text{ V}$ . The effect that explains the first behavior is related to the effective mobility changing with  $V_B$ , which will be detailed in Section 3.1. The second effect happens due to  $V_{\text{TH}}$  mismatch, the closer both threshold voltages get, the higher the transconductance, once both conduction are overlapped from their starting point, where no strong mobility degradation is observed yet due to surface roughness.

Fig. 2c confirms the existence of  $V_{\text{TH}}$  mismatch between top and bottom levels at  $V_B = 0 \text{ V}$ . The constant peak in Fig. 2c is insensitive to  $V_B$  and related to the threshold voltage of the top NW ( $V_{\text{TH,GAA}}$ ), while the other one is sensitive to  $V_B$  and corresponds to the threshold voltage of the bottom  $\Omega$ -NW ( $V_{\text{TH,}\Omega\text{G}}$ ). No peak is observed due to back conduction because of its small contribution, as indicated in Fig. 2a and expected in narrow  $\Omega$ -NWs.  $V_{\text{TH}}$  mismatches could be related to charge traps in the GAA-NW, which presents much lower  $V_{\text{TH}}$  and is more susceptible to defects after RMG process fabrication in comparison to the bottom level.

Fig. 3 shows threshold voltage,  $V_{\text{TH}}$  (a), and subthreshold slope, S (b), as a function of  $V_B$  for stacked NWs with  $W_{\text{FIN}} = 15$  and  $25 \text{ nm}$  and  $L = 100 \text{ nm}$ , at  $V_{\text{DS}} = -40 \text{ mV}$ . The threshold voltage has been extracted by the double derivative method. The subthreshold slope has been extracted from  $\partial V_{\text{GS}} / \partial (\log I_{\text{DS}})$  curves, considering an average around the minimum value to account for  $\sim 1$ – $2$  decades of  $I_{\text{DS}}$ . Fig. 3a presents  $V_{\text{TH}}$  for both bottom ( $V_{\text{TH,}\Omega\text{G}}$ ) and top ( $V_{\text{TH,GAA}}$ ) NWs extracted from  $\delta g_m / \delta V_{\text{GS}}$  peaks in Fig. 2c. Threshold voltage mismatches between bottom and top NWs are found to be  $0.32$  and  $0.34 \text{ V}$  for  $W_{\text{FIN}} = 15$  and  $25 \text{ nm}$ , respectively, at  $V_B = 0 \text{ V}$ . It is observed that  $V_{\text{TH,}\Omega\text{G}}$  exhibits a plateau for  $V_B < -10 \text{ V}$  because the back interface of the bottom NW operates in inversion, which degrades the overall subthreshold slope. For  $V_B > -10 \text{ V}$ , the bottom NW enters in full depletion and  $V_{\text{TH,}\Omega\text{G}}$  decreases linearly with  $V_B$  increase, while  $V_{\text{TH,GAA}}$  remains constant once the top NW is  $V_B$  independent. Due to thin silicon layer, the bottom NW never reaches accumulation [14]. At  $V_B = 50 \text{ V}$ ,  $V_{\text{TH,}\Omega\text{G}} = V_{\text{TH,GAA}}$ . The NW level with lower  $|V_{\text{TH}}|$  conducts at lower  $|V_{\text{GS}}|$  and, therefore, dominates the subthreshold slope behavior of the overall structure. The  $I_{\text{DS}}$  of the NW level with higher  $|V_{\text{TH}}|$  is orders of magnitude lower comparing to the other NW level, at a given  $V_{\text{GS}}$  in the subthreshold regime, so its subthreshold characteristic is hidden in the I-V curve of the overall structure. For  $V_B > 50 \text{ V}$ ,  $|V_{\text{TH,}\Omega\text{G}}| > |V_{\text{TH,GAA}}|$ , thus the subthreshold characteristics observed in  $I_{\text{DS}}$  are determined by the GAA-NW. This explanation is consistent with constant S results varying  $V_B$  above  $50 \text{ V}$ , because GAA characteristics are independent of  $V_B$ .

### 2.2. Non-stacked $\Omega$ -NWs

Once the overall behavior of the stacked structure varying  $V_B$  is

Download English Version:

<https://daneshyari.com/en/article/10127497>

Download Persian Version:

<https://daneshyari.com/article/10127497>

[Daneshyari.com](https://daneshyari.com)